

RESEARCH BRIEF

Epigenetic Suppression of Transgenic T-cell Receptor Expression via Gamma-Retroviral Vector Methylation in Adoptive Cell Transfer Therapy

Theodore S. Nowicki^{1,2,3}, Colin Farrell⁴, Marco Morselli^{5,6}, Liudmilla Rubbi⁶, Katie M. Campbell⁷, Mignonette H. Macabali⁷, Beata Berent-Maoz⁷, Begoña Comin-Anduix^{2,8}, Matteo Pellegrini^{2,5,6}, and Antoni Ribas^{2,3,7,8,9}

ABSTRACT

Transgenic T-cell receptor (TCR) adoptive cell therapies recognizing tumor antigens are associated with robust initial response rates, but frequent disease relapse. This usually occurs in the setting of poor long-term persistence of cells expressing the transgenic TCR, generated using murine stem cell virus (MSCV) γ -retroviral vectors. Analysis of clinical transgenic adoptive cell therapy products *in vivo* revealed that despite strong persistence of the transgenic TCR DNA sequence over time, its expression was profoundly decreased over time at the RNA and protein levels. Patients with the greatest degrees of expression suppression displayed significant increases in DNA methylation over time within the MSCV promoter region, as well as progressive increases in DNA methylation within the entire MSCV vector over time. These increases in vector methylation occurred independently of its integration site within the host genomes. These results have significant implications for the design of future viral vector gene-engineered adoptive cell transfer therapies.

SIGNIFICANCE: Cellular immunotherapies' reliance on retroviral vectors encoding foreign genetic material can be vulnerable to progressive acquisition of DNA methylation and subsequent epigenetic suppression of the transgenic product in TCR adoptive cell therapy. This must be considered in the design of future generations of cellular immunotherapies for cancer.

INTRODUCTION

Genetically engineered adoptive cell therapy (ACT) is revolutionizing cancer treatment, with sustained clinical responses seen in a variety of malignancies. Current approaches utilize

retroviral or lentiviral vectors for *ex vivo* transduction of a patient's T cells to express either a cancer antigen-specific T-cell receptor (TCR) or a chimeric antigen receptor (CAR). These reinfused cells then create a focused antitumor response in a variety of cancer subtypes (1, 2). However, although these

¹Division of Pediatric Hematology-Oncology, Department of Pediatrics, University of California, Los Angeles, Los Angeles, California. ²Jonsson Comprehensive Cancer Center, University of California, Los Angeles, Los Angeles, California. ³Eli and Edythe Broad Center for Regenerative Medicine and Stem Cell Research, University of California, Los Angeles, Los Angeles, California. ⁴Department of Human Genetics, University of California, Los Angeles, Los Angeles, California. ⁵Institute for Quantitative and Computational Biosciences – The Collaboratory, University of California, Los Angeles, Los Angeles, California. ⁶Department of Molecular, Cell, and Developmental Biology, University of California, Los Angeles, Los Angeles, California. ⁷Division of Hematology-Oncology, Department of Medicine, University of California, Los Angeles, Los Angeles, California. ⁸Division of Surgical Oncology, Department of Surgery, University of California, Los Angeles, Los Angeles, California.

⁹Department of Molecular and Medical Pharmacology, University of California, Los Angeles, Los Angeles, California.

Note: Supplementary data for this article are available at Cancer Discovery Online (<http://cancerdiscovery.aacrjournals.org/>).

Corresponding Author: Theodore S. Nowicki, University of California, Los Angeles, 12-159 Factor Building, 10833 Le Conte Avenue, Los Angeles, CA 90095. Phone: 310-825-6708; Fax: 310-206-8089; E-mail: tnowicki@mednet.ucla.edu

Cancer Discov 2020;10:1645-53

doi: 10.1158/2159-8290.CD-20-0300

©2020 American Association for Cancer Research.

treatments lead to durable clinical responses in many patients, a significant number of patients remain who do not respond, or who eventually relapse. Previous ACT clinical trials conducted by our group and others against the tumor antigens MART-1 (in melanoma) and NY-ESO-1 (in sarcoma and melanoma) have demonstrated that detectable surface expression of the transgenic TCR is rapidly lost in circulating T cells following infusion (3–6). The transduction of these cells relies on retroviral vectors, most commonly the murine stem cell virus (MSCV), a γ -retrovirus which has been optimized for highly efficient transgene expression and has been used for a variety of such applications *in vivo* (7). However, it has subsequently been shown to be vulnerable to epigenetic silencing via DNA methylation of CpG loci which are clustered within its 5' long tandem repeat (LTR) promoter region (8, 9).

Given our observation of this phenomenon of rapid loss of surface expression of the transgenic TCR in circulating T cells *in vivo*, along with the vulnerability of the MSCV vector to epigenetic silencing via DNA methylation, we hypothesized that acquisition of DNA methylation within the retroviral 5'LTR promoter was associated with loss of expression of the transgenic TCRs in these clinical samples. Herein, we describe the analysis of clinical transgenic ACT samples for persistence of the transgenic TCR DNA sequence and accompanying expression of the TCR itself, as well as characterizing the DNA methylation status of the MSCV vector over time, and the relationship between vector methylation and suppression of transgenic TCR expression.

RESULTS

Trial Conduct, Patient Characteristics, and Outcomes

Sixteen patients from our previous transgenic TCR ACT trials directed against MART-1 (4) and NY-ESO-1 (5) were selected for analysis. Patient demographics, clinical characteristics, and outcomes are summarized in Table 1. Following conditioning chemotherapy, patients were all treated with up to 1×10^9 autologous transgenic TCR T cells, which were generated via *ex vivo* transduction using the MSCV γ -retrovirus encoding the F5-MART-1 TCR or the NY-ESO-1 TCR (Supplementary Fig. S1). Of the 16 patients selected, 7 of 8 patients treated with F-5 MART-1 TCR transgenic T cells and 6 of 8 patients treated with NY-ESO-1 TCR transgenic T cells demonstrated a transient objective response to therapy.

Transgenic TCR-Engineered T Cells Display Strong Persistence of the Transgene DNA Sequence, but with Greatly Reduced Expression of the RNA and Surface Protein over Time

The above-mentioned 16 patients had peripheral mononuclear blood cell (PBMC) samples from both their infusion (day 0) and 70 days after treatment (in peripheral circulation) analyzed for persistence of the transgenic TCR and RNA and surface TCR protein expression. All infusion products demonstrated robust presence of the transgenic TCR gene and its RNA and surface protein expression. However, we observed that despite largely decreased expression of the RNA transcript and the surface protein at day +70, persistence of the transgenic

TCR still accounted for the vast majority of circulating TCR DNA clonotypes as measured by TCR sequencing using the ImmunoSEQ platform (Fig. 1A; Supplementary Figs. S1–S3). The lowest tertile of TCR surface protein expression ($n = 6$) was noted to have <0.5% surface TCR protein expression of circulating CD3⁺ cells, the threshold previously established as a highly expanded clone (10, 11). These 6 patients were designated as an “expression-low” cohort for further analyses, whereas the remaining 10 patients were designated as “expression-high.” Although the expression-high cohort demonstrated correlation between transgenic TCR DNA and protein proportions when analyzed by linear regression, this correlation was not observed in the expression-low cohort (Supplementary Fig. S4A and S4B). Although the degree of RNA and surface protein expression of the transgenic TCRs was significantly lower at day +70 in the expression-low group compared with the expression-high group, there were no statistically significant differences between the two cohorts' proportion of transgenic TCR DNA in circulating PBMCs at day +70, which still accounted for the majority of circulating TCR clonotypes (Fig. 1B–D; Supplementary Figs. S5 and S6). There were also no statistically significant differences between the two groups' transgenic TCR proportions and surface protein expression at day 0 (Supplementary Fig. S7A and S7B).

Increased MSCV 5'LTR Methylation Is Associated with Decreased Expression of the Transgenic RNA and Protein, Despite Persistence of the Transgenic DNA

Given the overall strong predominance of transgenic TCR representation within the TCR repertoire of circulating T cells despite profound loss of its expression, we explored the degree of CpG methylation within the MSCV 5'LTR promoter region, which contains a CpG island characterized by a high concentration of clustered CpG loci over a relatively small region of DNA (Fig. 2A). Genomic DNA was isolated from PBMCs from each patient sample at baseline (day 0) and 70 days after infusion and bisulfite-converted. The area of DNA within the MSCV 5'LTR containing the CpG island was amplified by PCR, purified, and sequenced. We found that although all day 0 infusion products contained relatively little CpG methylation within the 5'LTR promoter region of the MSCV vector, the 6 patients in the expression-low cohort individually demonstrated significantly increased levels of CpG methylation at day +70 (Fig. 2B and C; Supplementary Figs. S8 and S9). The average proportion of promoter methylation was anticorrelated with transgenic TCR surface protein expression among all patients at day +70 (Supplementary Fig. S10). Furthermore, when the two cohorts were compared with one another, the expression-low cohort displayed significantly greater CpG methylation within the 5'LTR promoter region when compared with the expression-high cohort at day +70 (Fig. 2D). Although there were no differences in progression-free survival or overall survival between the two cohorts, the expression-low cohort displayed an inferior decrease in tumor burden compared with the expression-high cohort, which nearly achieved statistical significance ($P = 0.07$; Supplementary Fig. S11A and S11B).

Table 1. Patient demographics and outcomes

| Patient study number | Sex (M/F) | Ethnicity | Age | Type of cancer | Active disease sites | Stage | Number of TCR transgenic cells | IL2 doses | DC doses | Evidence of transient tumor response | Response at EOS (day 90) | PFS (mo) | OS (mo) | Current status |
|----------------------|-----------|-----------|-----|------------------|---|-------|--------------------------------|-----------|----------|--------------------------------------|--------------------------|----------|---------|-----------------|
| F5-1 | M | Caucasian | 60 | Melanoma | Lung, stomach, liver, pancreas, peritoneum, soft tissues | M1c | 1×10^9 | 12/14 | 3/3 | Yes by PET/CT | PD | 3 | 5 | Died of disease |
| F5-3 | M | Caucasian | 61 | Melanoma | Lung, liver | M1c | 1×10^9 | 13/14 | 3/3 | Yes by PET/CT | SD | 7 | 86 | Died of disease |
| F5-6 | M | Caucasian | 59 | Melanoma | Lung, LN | M1b | 1×10^9 | 13/14 | 3/3 | Yes by PE | SD | 3 | 4 | Died of disease |
| F5-7 | M | Caucasian | 48 | Melanoma | SC, bone | M1c | 1×10^9 | 9/14 | 3/3 | Yes by CT | SD | 4 | 11 | Died of disease |
| F5-8 | M | Caucasian | 44 | Melanoma | LN, liver | M1c | 1×10^9 | 11/14 | 3/3 | Yes by PET/CT | SD | 4 | 11 | Died of disease |
| F5-9 | F | Caucasian | 46 | Melanoma | Skin, LN | M1a | 1×10^9 | 11/14 | 3/3 | No | PD | 3 | 20 | Died of disease |
| F5-12 | M | Caucasian | 40 | Melanoma | Lung, LN | M1Vb | 3.9×10^9 | 6/9 | 3/3 | Yes by PET/CT | SD | 5 | 8 | Died of disease |
| F5-13 | M | Caucasian | 60 | Melanoma | Lung, abdomen, SC | M1Ib | 4.41×10^9 | 4/9 | 3/3 | Yes by PET/CT | SD | 3 | 8 | Died of disease |
| ES0-1 | M | Hispanic | 47 | Liposarcoma | Right renal fossa; liver left lobe; hepatic segment; peritoneal, perihepatic nodule | IV | 7.7×10^8 | 28/28 | 3/3 | No | PD | 2.6 | 16 | Died of disease |
| ES0-3 | F | Caucasian | 24 | Synovial sarcoma | Right lung; multiple pulmonary nodules | IV | 1×10^9 | 19/28 | 1/3 | Yes by PET/CT | PR | 67 | 67 | Alive with CR |
| ES0-4 | M | Caucasian | 41 | Synovial sarcoma | Left infraclavicular mass; left pectoralis mass | III | 1×10^9 | 18/28 | 3/3 | Yes by PET/CT | PD | 3 | 25 | Died of disease |
| ES0-5 | F | Caucasian | 43 | Synovial sarcoma | Right popliteal fossa; lung | IV | 1×10^9 | 14/14 | 3/3 | Yes by PET/CT | PR | 9 | 41.5 | Died of disease |
| ES0-6 | M | Caucasian | 26 | Osteosarcoma | Lung | IV | 1×10^9 | 14/14 | 3/3 | Yes by PET/CT | PD | 2.5 | 19 | Died of disease |
| INY-2 | M | Caucasian | 66 | Melanoma | LN, liver | IV | 1×10^9 | 21/28 | 2/3 | Yes by PET/CT | PD | 3 | 6 | Died of disease |
| INY-3 | F | Caucasian | 44 | Synovial sarcoma | Right popliteal fossa; lung | IV | 1×10^9 | 14/14 | 3/3 | Yes by PET/CT | PD | 3 | 31 | Died of disease |
| INY-4 | M | Hispanic | 24 | Melanoma | Lung, LN, adrenal gland, liver, trachea, brain | IV | 1×10^9 | 10/14 | 3/3 | No | PD | NA | 3 | Died of disease |

Abbreviations: CR, complete response; DC, dendritic cells; EOS, end of study; F, female; LN, lymph nodes; M, male; mo, months; OS, overall survival; PD, progressive disease; PFS, progression-free survival; PR, partial response; SC, subcutaneous; SD, stable disease.

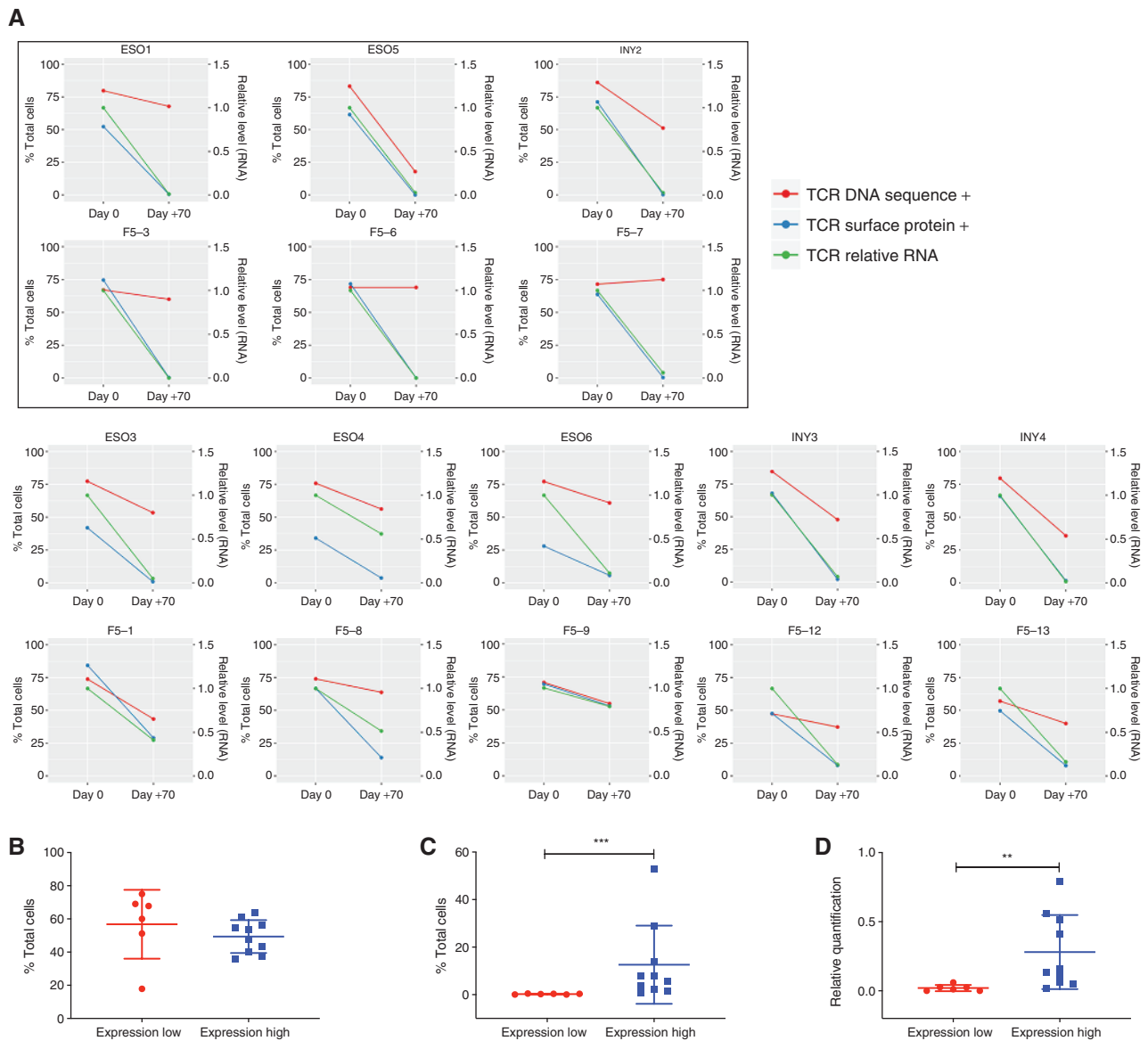


Figure 1. Persistence of transgenic TCR DNA and RNA/protein expression of TCR-engineered T cells over time. **A**, Comparison between infusion products (day 0) and postinfusion recovery products 70 days later from patients on NYESO-1 TCR-engineered cell therapy trials (ESO and INY) or F5-MART-1 TCR-engineered cell therapy trial (F5). Data displayed are percentage of cells containing the transgenic TCR DNA sequence via TCR sequencing (red, left axis), the percentage of cells expressing the TCR protein via MHC dextramer FACS (green, left axis), and the relative level of RNA transcript via qRT-PCR (blue, right axis). Inset boxed patients represent those with surface TCR expression <0.5% at day +70 (expression-low). **B-D**, Statistical comparisons between expression-high and expression-low patient cohorts demonstrating no significant differences between day +70 transgenic TCR DNA (**B**), whereas surface protein expression (**C**) and relative RNA level (**D**) at day +70 are significantly lower in the expression-low cohort (**, $P < 0.01$; ***, $P < 0.001$, Mann-Whitney U test).

CpG Methylation Is Increased across MSCV Vector over Time in All Patients and Is Significantly Greater in Those with Decreased Transgenic TCR Expression over Time

In order to expand our ability to characterize CpG methylation across the entire MSCV vector over time, we performed bisulfite conversion on genomic DNA library preparations isolated from all patients' PBMC samples at day 0 (infusion), day +30, and day +70. We then carried out target enrichment using RNA probes to capture the MSCV vector. Bisulfite-converted libraries were then aligned against the human

genome version 38 (hg38) with MSCV transgenic TCR vector reference sequences utilizing BSBolt, an integrated alignment and analysis platform for bisulfite-converted DNA. Each patient sample demonstrated overall progressive increases in CpG methylation across the transgenic TCR MSCV vector sequence over time (Fig. 3A and B). When all patient sample data were aggregated, the increases in MCV vector CpG methylation were statistically significant at day +30 compared with day 0, and day +70 compared with day +30 (Fig. 3C). When the data were further stratified to compare the expression-high and expression-low patient cohorts, we observed that

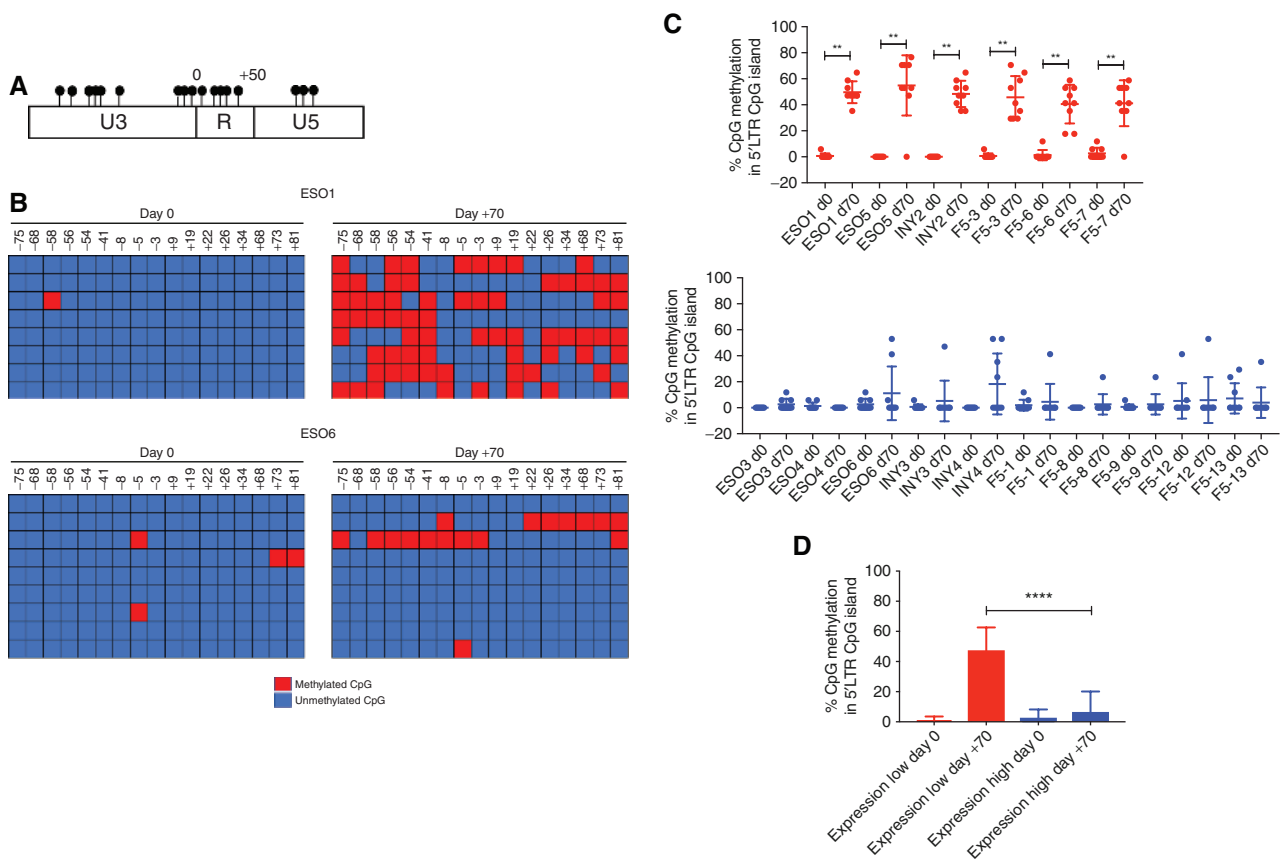


Figure 2. Increased MSCV 5'LTR methylation is associated with decreased expression of the transgenic RNA and protein, despite persistence of the transgenic DNA. **A**, CpG island within the MSCV 5'LTR, where each CpG loci is represented by a filled circle. Numbering is relative to the TSS. **B**, Bisulfite conversion was performed on genomic DNA from patient PBMCs at day 0 (infusion) and day +70, and the CpG island within the MSCV 5'LTR promoter region was PCR amplified and purified; 2 representative patients are shown. Each row represents sequencing of an individual experiment, with methylated cytosine loci indicated by red boxes and unmethylated loci by blue boxes. CpG loci positions are listed at the top of the graph relative to the TSS for the transgenic TCR. **C**, Percentage of CpG methylation within 5'LTR at day 0 and day +70 in individual expression-low (red) and expression-high (blue) patients (**, $P < 0.01$, Wilcoxon matched-pairs signed rank test); comparison between aggregate percent CpG methylation within the 5'LTR between all expression-high and expression-low patients at day 0 and day +70 is shown in **D** (****, $P < 0.0001$, Mann-Whitney U test).

although there were no significant differences between baseline levels of CpG methylation at day 0, the day +30 and day +70 methylation ratios, which progressively increased over time in both cohorts, were significantly higher in the expression-low cohort when compared with the expression-high cohort, consistent with what was observed in the targeted analysis of the 5'LTR promoter region (Fig. 3D).

MSCV-TCR Vector Integration Occurs Sporadically throughout the Host Genome Relative to Transcription Start Sites

While capturing the MSV vector fragments, we also obtained fragments that spanned the junction of the insertion site between the vector and the genome. These reads allowed us to explore the integration patterns of the MSCV vector within the patients' genomes. Specifically, we utilized BSBolt to map discordant paired reads, where individual reads from the pair map to both the human genome and the MSCV transgenic TCR vector. Integration sites were characterized by their relative and absolute distance to transcription start sites (TSS). We observed that the MSCV vector integration sites occurred at sites generally distal to gene TSS

(Supplementary Fig. S12A and S12B). Furthermore, when we compared the proportions of vector integration sites by their relative distance to TSS, we observed no significant differences between the expression-low cohort (i.e., those with high CpG methylation levels) and the expression-high cohort (i.e., those with low CpG methylation levels), suggesting that the integration site relative to TSS did not affect the degree of CpG methylation observed within a given vector read.

DISCUSSION

TCR transgenic ACT has established itself as a potent form of cancer immunotherapy for a wide variety of tumor subtypes. However, despite frequent early responses and reduction in tumor burden, the durability of these responses is often poor, and tumors often progress within several months. Our clinical experiences with transgenic TCR ACT generated with γ -retroviral vectors, as well as those of other groups, have consistently demonstrated that the presence of detectable circulating transgenic TCR surface expression rapidly diminishes within 1 to 2 months following cell transfer, in keeping with the timeline of disease progression after the initial transient

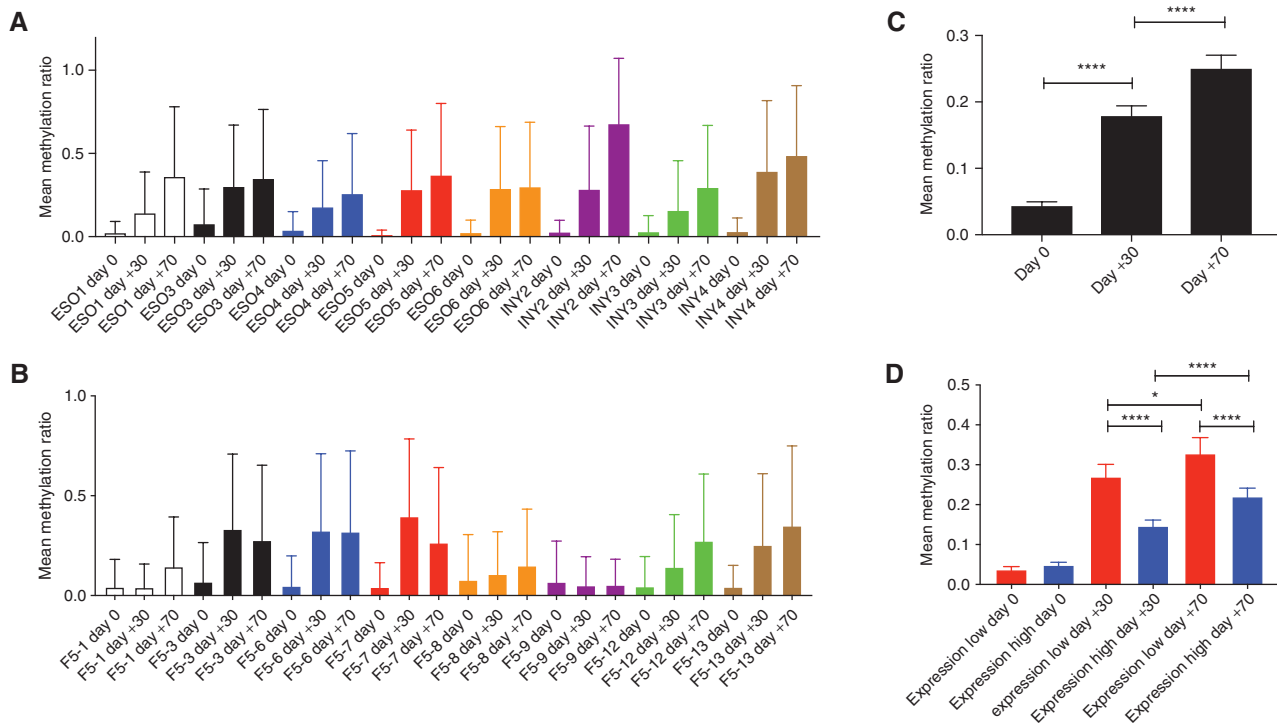


Figure 3. CpG methylation is increased across MSCV vector over time in all patients and is significantly greater in those with decreased transgenic TCR expression over time. Mean methylation ratio across MSCV vector at day 0, day +30, and day +70 for each patient treated with NY-ESO-1 TCR (A) and F5-MART-1 TCR (B) transgenic T cells. C, Statistical comparisons between methylation values in all patients at day 0, day +30, and day +70; data are stratified to compare the increases in methylation values over time between the expression-high and expression-low patients in D (*, $P < 0.05$; ****, $P < 0.0001$, Mann-Whitney U test).

response to therapy (3–6). This is in stark contrast to ACT using autologous cancer antigen-specific TCR clones, which are isolated, expanded *ex vivo*, and reinfused to the patient without the aid of any viral vectors to transduce and generate these cells in large numbers. Previous ACT studies utilizing such endogenous TCR clones have shown remarkably strong persistence of cancer antigen-specific TCR clones in circulation following cell transfer (12, 13). This discrepancy implies that genetically engineered ACT products have a fundamental vulnerability in the suppression of their transgenic TCR.

Given the known vulnerability of the MSCV vector to epigenetic silencing via CpG methylation, as well as the observed discordance between the strong persistence of the TCR transgenes and their poor expression in circulation, we hypothesized that increases in DNA methylation within the vector were associated with this phenomenon. Although one small series of patients previously found no significant retroviral promoter methylation to cause suppression of transgenic TCR expression (14), that study only examined the methylation status of the MSCV vector promoter in a total of 4 patients. Our examination of 16 samples from patients receiving transgenic ACT demonstrated that samples from only 6 of these patients displayed significantly discordant, profound decreases in expression of the transgenic TCR which was associated with significant increases in MSCV vector methylation. This suggests that the phenomenon occurs in a minority of patients and could be missed by sampling too small a cohort. Indeed, there may be cell phenotype-specific or patient-specific predispositions to rapid acquisition of CpG methylation of γ -retroviruses which would not

be present in every subject studied. Although further detailed studies of factors such as patient-specific polymorphisms in DNA methyltransferase enzymes would be needed to derive even speculative inferences into such predispositions, our studies did not demonstrate any significant association with the MSCV integration site's distance to a given TSS at infusion and its propensity to acquire CpG methylation over time. Furthermore, our characterization of the MSCV vector integration sites was consistent with previously published studies dealing with the γ -retroviral vector murine leukemia virus, which showed that only approximately 25% of γ -retrovirus integration sites are within ± 2.5 kb of the TSS (15) in human cells, consistent with our results. Although MSCV has previously shown increased integration near TSS in murine bone marrow cells (16), it may be that there are species-specific factors which influence integration site, as our data are consistent with previously published data in humans.

The vulnerability of retroviral vectors to epigenetic suppression in transgenic TCR ACT products seen here raises an important question about how to overcome this potential weakness in clinical practice. One possibility would be to utilize dual therapy with systemic hypomethylating agents such as decitabine to prevent the acquisition of CpG methylation within the retroviral vector encoding the transgenic TCR. Such agents have also been shown in murine models to increase the expression of tumor antigens commonly targeted by transgenic TCR ACT, such as NY-ESO-1 (17, 18), theoretically further enhancing the immunotherapeutic effect of the transgenic T cells. However, DNA methylation

is often followed by histone recruitment and modification (deacetylation and/or methylation), which further contribute to epigenetic suppression. Therefore, such pharmacologic interventions would potentially be insufficient to fully reverse epigenetic suppression, as it would not have an effect on the histone modifications and recruitment. Stimulation of T cells with IL2 and anti-CD3/CD28 beads has previously been shown to partially restore transgenic TCR expression *in vitro* in some patients, likely due to nonspecific modulation of these epigenetic factors (14). New nonviral approaches to generating transgenic TCR T cells using CRISPR/Cas9 to deliver constructs under control of the native TCR promoter (rather than a viral promoter) would also potentially avoid this risk of epigenetic suppression of viral vector–encoded products (19). Furthermore, there may be utility in new modalities that provide a continuous supply of transgenic T cells to the patient. Preclinical models have demonstrated that CD34⁺ hematopoietic stem cells encoding a transgenic TCR can endogenously differentiate into fully functional T cells expressing the TCR (20, 21). We currently have an open phase I clinical trial which utilizes this approach against NY-ESO-1 in solid tumors (NCT03240861), utilizing a lentiviral stem cell transduction for long-term expression.

One major limitation of our study is that we only examined transgenic TCR ACT products generated using the MSCV γ -retrovirus, which is known to be potentially vulnerable to epigenetic silencing via CpG methylation. Other types of cell therapy products, including the CD19 CAR-T product Kymriah (tisagenlecleucel), utilize lentiviral vectors, which have previously demonstrated remarkable persistence of transgene expression *in vivo* and do not appear vulnerable to CpG methylation (22), which may limit the broader applicability of our findings. Indeed, transgenic TCR ACT products manufactured using lentiviral vectors have been shown to have far superior persistence of detectable surface expression of the TCR (23). Although the other commercially available CD19 CAR-T product Yescarta (axicabtagene ciloleucel) does utilize a γ -retroviral vector for its manufacture, its rates of durable complete and partial remission are far superior to any published transgenic TCR product (2). This is likely due to the rapid systemic clearance of lymphoma cells seen when using these ACT products, implying that long-term persistence of the transgenic T cells in this setting is potentially less important than in treating refractory solid tumors with such therapeutics. Indeed, our examination of patient samples at day +70 was chosen due to this being the average point of circulating transgenic T-cell nadir in our previously published trials (4, 5). We were unable to determine any association of γ -retroviral vector methylation with patient survival, likely owing to the overall small number of long-term responders inherent to this therapy in solid tumors.

In summary, we have shown that progressive increases in CpG methylation within the MSCV γ -retroviral vector are associated with rapid suppression of transgenic TCR expression over time in clinical transgenic ACT, despite strong persistence of the transgene itself. This phenomenon did not appear to have any correlation with vector integration site within the host genome. These findings have significant implications in how the cellular therapeutics community should approach the design of future generations of these products.

METHODS

Clinical Trial, Patients, and Manufacturing of MART-1 and NY-ESO-1 TCR Engineered T Cells

For the F5-MART-1 transgenic TCR ACT clinical trial, patients positive for HLA-A*0201 with a MART-1–positive metastatic melanoma were enrolled under NCT00910650 [UCLA Institutional Review Board (IRB) #08-02020 and #10-001212] from April 2009 to September 2011, under investigational new drug (IND) #13859 (4). For the NYESO-1 transgenic TCR ACT clinical trials, patients positive for HLA-A*0201 with an NYESO-1–positive sarcoma or melanoma were enrolled under NCT02070406 or NCT01697527 (UCLA IRB #12-000153 and #13-001624, respectively) under IND #15167 (5). Written informed consent was obtained from all patients, and studies were conducted in accordance with local regulations, the guidelines for Good Clinical Practice, and the principles of the Declaration of Helsinki. All studies were approved by the UCLA IRB under the above approval numbers. Clinical trial design and manufacturing of the MART-1 and NYESO-1 TCR transgenic T cells were previously described (4, 5). Briefly, nonmobilized autologous PBMCs were stimulated in culture with IL2/OKT3 and transduced with clinical grade MSCV retrovirus vector expressing the MART-1 F5 TCR or the NYESO-1 TCR on 2 consecutive days, and then continually expanded *ex vivo* for 6 to 7 days. Up to 1×10^9 transgenic TCR transgenic lymphocytes were administered to each patient following conditioning chemotherapy with cyclophosphamide and fludarabine, along with postinfusion systemic IL2 for 7 to 14 days, and dendritic cell vaccine boosts, as previously described (4, 5).

Quantification of Transgenic TCR β Genomic DNA Persistence

Genomic DNA and RNA were isolated from patient-matched infusion products and postinfusion PBMCs recovered at day +70 (± 10 days), with an AllPrep DNA/RNA isolation kit according to the manufacturer's instructions (Qiagen). TCR β alleles were sequenced at 100,000 reads by Adaptive Biotechnologies. Bulk TCR sequencing was utilized due to its superior sampling depth (previously characterized as 20-fold greater) and sensitivity over single-cell RNA sequencing–based approaches in detection of nontransgenic TCR clonotypes (24). Briefly, this process utilizes a synthetic immune repertoire, corresponding to every possible biological combination of Variable (V) and Joining (J) gene segments for each TCR locus, spiked into every sample at a known concentration. These inline controls enable rigorous quality assurance for every sample assayed and allow for correction of multiplex PCR amplification bias, providing an absolute quantitative measure of T cells containing the transgenic TCR relative to the other endogenous TCR clonotypes, with no difference in amplification efficiency (25). Productive TCR β sequences, i.e., those that could be translated into open reading frames and did not contain a stop codon, were reported. The transgenic F5-MART-1 and NY-ESO-1 TCR sequences' persistence was identified based on comparison of reads with the known TCR β sequence for the transgenic product, and expressed as a percentage of total productive TCR β sequences present within a given sample/timepoint.

qRT-PCR

Total RNA isolated from patient samples (as described above) was used for analysis of relative abundance of the transgenic F5 MART-1 TCR or the NYESO-1 TCR. Samples were converted to cDNA using iScript TM Reverse Transcription Supermix for RT-PCR (Bio-Rad), and then cDNA was amplified and quantified using iTaq TM Universal SYBR Green Supermix (Bio-Rad) on an Applied Biosystems 7500 Fast Real-Time PCR System (Applied Biosystems). PCR conditions were 1 cycle of 1 minute at 95°C, 35 cycles of 15 seconds at 95°C and 60 seconds at 60°C, and 5-minute incubation at 72°C. Replicate samples were run with test primer sets for the F5-MART-1 TCR, the NYESO-1 TCR, or the endogenous control GAPDH; primer sequences are available upon request. Data were analyzed according to the comparative Ct method.

MHC Dextramer Immunologic Monitoring for Surface Expression of Transgenic TCRs

Detection and quantification of F5 MART-1 TCR or NY-ESO-1 TCR expression using fluorescent MHC dextramer analysis for MART-1 or NY-ESO-1 (Immudex) was performed on patient-matched infusion products and postinfusion PBMCs recovered at day +70, as previously described (4, 5, 26). Our definitions for a positive or negative immunologic response using standardized MHC multimer assays were used, which are based on assay performance specifications by defining changes beyond the assay variability with a 95% confidence level (26).

Bisulfite Sequencing of MSCV Retroviral Promoter in Patient Samples

Genomic DNA isolated from patient PBMC samples was bisulfite converted using the EZ DNA Methylation-Gold Kit (Zymo Research) according to the manufacturer's instructions. A CpG island within the MSCV 5'LTR promoter U3/R/U5 region, defined as an area >100 bp, with a GC content of >50%, and possessing an observed:expected CpG ratio of >0.6, was determined using MethPrimer software (27), which also designed PCR primers capable of amplifying the methylated and nonmethylated bisulfite-converted DNA sequence of interest. CpG islands were PCR amplified, purified, and subjected to DNA Sanger sequencing (Laragen). The methylation status of each CpG locus within the individual amplicons was determined using QUMA software (28).

Targeted Bisulfite Sequencing Library Preparation and Sequencing

Purified genomic DNA from patient samples (isolated as described above) was quantified using the Qubit dsDNA BR Assay (Thermo Fisher Scientific). For each sample, 250 ng of DNA was sonicated using a Bioruptor Pico (Diagenode) for 15 cycles (30 seconds ON; 60 seconds OFF). Libraries were prepared using the NEBNext Ultra II DNA kit (NEB) according to the manufacturer's instructions with few modifications. Briefly, sonicated DNA was subjected to EndPrep (End Repair and A-tailing), followed by Adapter Ligation using 2.5 μ L of Illumina TruSeq premethylated Adapters (Illumina). Samples were purified using 0.85x NEB Purification Beads and eluted in 15 μ L of 10 mmol/L Tris-HCl, pH 8. Samples were mixed in 16-sample pools and column purified using a DCC-5 (Zymo Research). Elution was performed with 10 μ L of 60°C 10 mmol/L Tris-HCl, pH 8. Each sample pool was subject to hybrid capture with custom biotinylated RNA probes designed to tile the MSCV vector (MyBaits Arbor Bioscience - Human_6K and Human_patch2) according to the manufacturer's protocol. The hybridization was carried out for 20 hours overnight at 65°C. Captured DNA was eluted by heating in 20 μ L of 10 mmol/L Tris-HCl pH 8+0.05% Tween-20. The eluted DNA was then subject to bisulfite conversion using the DNA Methylation Lightning Kit (Zymo Research). Converted DNA was then amplified using xGen Library Amplification Primer Mix (IDT) and Kapa Uracil+ Ready Mix using the following conditions: 98°C for 2 minutes; 20 cycles of 98°C for 20 seconds, 60°C for 30 seconds, 72°C for 30 seconds; Final Extension 72°C for 5 minutes; hold 4°C. PCR products were purified using 0.9 volumes of NEBNext Purification Beads and eluted in 15 μ L of 10 mmol/L Tris-HCl, pH 8. Final libraries were then quantified using the Qubit dsDNA BR Assay (Thermo Fisher Scientific) and visualized using a D1000 ScreenTape (TapeStation 2200 system - Agilent Technologies). Each pool was then sequenced at 150 bp PE on a HiSeq 3000 instrument (Illumina).

Targeted Bisulfite Sequencing Alignment and Methylation Calling

Paired end, 150-bp targeted bisulfite sequencing reads were aligned to the combined hg38 and MSCV transgenic TCR vector sequence bisulfite-converted references using BSBolt v0.1.2 (<https://github.com/NuttyLogic/BSBolt>) local alignment. Alignments with <5 mismatches and an alignment score >160 were considered valid, and up to 10 alignments per read pair were considered. Alignments where read

pairs did not meet expected paired end constraints, an insert size >500 bp, or alignments on separate chromosomes, were reported as discordant. Read pairs with only one valid alignment were reported as mixed. Duplicate reads were removed using SAMtools v1.9 (29). Following duplicate removal, methylation values were called for all observed cytosines with ≥ 5 reads with a base call quality above 25 using BSBolt v0.1.2 (<https://github.com/NuttyLogic/BSBolt>). Sequencing data were available in NCBI's Gene Expression Omnibus (accession number GSE153820).

Vector Integration Site Detection

Discordant read pairs with a vector alignment and a genome alignment were evaluated as potential integration sites. Discordant read pairs were further filtered by removing reads that aligned to genomic regions homologous with the vector sequence or aligned outside the expected integration region within the vector sequence. Alignments with an alignment score greater than 160 and with secondary alignments that repeated no more than 10% of the primary alignment sequence were considered integration site supporting alignments. Integration sites were reported as the closest genomic base to vector alignment or the average integration site position for sites with multiple supporting reads. The integration site selection pipeline was implemented using custom python code (<https://github.com/NuttyLogic/Epigenetic-suppression-of-transgenic-TCR-expression-in-ACT>). The vector integration detection pipeline was validated against simulated 150-bp, paired end bisulfite-converted vector integration libraries (see Supplementary Methods for further details).

Statistical Analysis

Graphing and descriptive statistical analyses were carried out with GraphPad Prism version 7.0 (GraphPad). Where indicated, Mann-Whitney *U* test or Wilcoxon matched-pairs signed rank test was used for comparison of two groups. Linear regression was performed comparing the correlation of transgenic TCR DNA and surface protein expression in the expression-high and expression-low cohorts (as the independent and dependent variables, respectively), as well as comparing CpG promoter methylation and transgenic TCR expression in all patient samples (as independent and dependent variables, respectively). *P* values of <0.05 were considered statistically significant.

Disclosure of Potential Conflicts of Interest

T.S. Nowicki reports personal fees from Allogene Therapeutics outside the submitted work. K.M. Campbell is a shareholder in Geneoscopy LLC. A. Ribas reports personal fees from Amgen, Chugai, Genentech, Jounce, Merck, Novartis, Nurix, Sanofi, Vedanta (honoraria from consulting), other from Advaxis, CytomX, Five Prime, RAPT, Isoplexis, Kite-Gilead (stock from prior SAB service), personal fees and other from 4C Biomed, Apricity, Arcus, Highlight, Compugen, ImaginAb, MapKure, Merus, Rgenix, Lutris, PACT Pharma, Tango (stock and honoraria from SAB membership), and grants from Agilent, Bristol-Myers Squibb (institutional grant support) outside the submitted work. No potential conflicts of interest were disclosed by the other authors.

Disclaimer

The contents of this article are solely the responsibility of the authors and do not necessarily represent the official views of the NIH, the NCI, The Eunice Kennedy Shriver National Institute of Child Health and Human Development (NICHD), the Parker Institute for Cancer Immunotherapy, or the Ressler Family Foundation.

Authors' Contributions

T.S. Nowicki: Conceptualization, Resources, Data Curation, Software, Formal Analysis, Supervision, Funding Acquisition, Validation, Investigation, Visualization, Methodology, Writing-Original Draft, Project Administration, Writing-Review and Editing. **C. Farrell:** Conceptualization, Data Curation, Software, Formal Analysis, Validation,

Investigation, Visualization, Methodology, Writing-Original Draft, Writing-Review and Editing. **M. Morselli:** Conceptualization, Formal Analysis, Validation, Investigation, Visualization, Methodology, Writing-Original Draft, Writing-Review and Editing. **L. Rubbi:** Conceptualization, Validation, Investigation, Visualization, Methodology. **K.M. Campbell:** Software, Formal Analysis, Validation, Investigation, Visualization, Methodology, Writing-Original Draft, Writing-Review and Editing. **M.H. Macabali:** Investigation. **B. Berent-Maoz:** Investigation. **B. Comin-Anduix:** Conceptualization, Formal Analysis, Validation, Investigation, Visualization, Methodology, Writing-Original Draft. **M. Pellegrini:** Conceptualization, Resources, Data Curation, Software, Formal Analysis, Supervision, Funding Acquisition, Methodology, Writing-Original Draft, Project Administration, Writing-Review and Editing. **A. Ribas:** Conceptualization, Resources, Funding Acquisition, Methodology, Writing-Original Draft, Project Administration, Writing-Review and Editing.

Acknowledgments

This study was funded in part by NIH grants R35 CA197633 and P01 CA168585, the Parker Institute for Cancer Immunotherapy, and the Ressler Family Fund (to A. Ribas). T.S. Nowicki is supported by the NIH/NICHD grant K12-HD000850 (Pediatric Scientist Development Program), the Tower Cancer Research Foundation Career Development Award, and the Hyundai Hope on Wheels Young Investigator Award. K.M. Campbell is supported by the UCLA Tumor Immunology Training Grant (NIH T32CA009120) and the Cancer Research Institute Irvington Postdoctoral Fellowship Program. Flow cytometry was performed in the UCLA Jonsson Comprehensive Cancer Center (JCCC) and Center for AIDS Research Flow Cytometry Core Facility that is supported by NIH awards P30 CA016042 and SP30 AI028697, and by the JCCC, the UCLA AIDS Institute, and the David Geffen School of Medicine at UCLA.

The costs of publication of this article were defrayed in part by the payment of page charges. This article must therefore be hereby marked *advertisement* in accordance with 18 U.S.C. Section 1734 solely to indicate this fact.

Received March 11, 2020; revised May 21, 2020; accepted July 7, 2020; published first July 22, 2020.

REFERENCES

- Yang JC, Rosenberg SA. Adoptive T-cell therapy for cancer. *Adv Immunol* 2016;130:279–94.
- June CH, Sadelain M. Chimeric antigen receptor therapy. *N Engl J Med* 2018;379:64–73.
- Morgan RA, Dudley ME, Wunderlich JR, Hughes MS, Yang JC, Sherry RM, et al. Cancer regression in patients after transfer of genetically engineered lymphocytes. *Science* 2006;314:126–9.
- Chodon T, Comin-Anduix B, Chmielowski B, Koya RC, Wu Z, Auerbach M, et al. Adoptive transfer of MART-1 T-cell receptor transgenic lymphocytes and dendritic cell vaccination in patients with metastatic melanoma. *Clin Cancer Res* 2014;20:2457–65.
- Nowicki TS, Berent-Maoz B, Cheung-Lau G, Huang RR, Wang X, Tsoi J, et al. A pilot trial of the combination of transgenic NY-ESO-1-reactive adoptive cellular therapy with dendritic cell vaccination with or without ipilimumab. *Clin Cancer Res* 2019;25:2096–108.
- Robbins PF, Kassim SH, Tran TLN, Crystal JS, Morgan RA, Feldman SA, et al. A pilot trial using lymphocytes genetically engineered with an NY-ESO-1-reactive T-cell receptor: long-term follow-up and correlates with response. *Clin Cancer Res* 2015;21:1019–27.
- Hawley RG, Lieu FH, Fong AZ, Hawley TS. Versatile retroviral vectors for potential use in gene therapy. *Gene Ther* 1994;1:136–8.
- Swindle CS, Kim HG, Klug CA. Mutation of CpGs in the murine stem cell virus retroviral vector long terminal repeat represses silencing in embryonic stem cells. *J Biol Chem* 2004;279:34–41.
- Yao S, Sukonnik T, Kean T, Bharadwaj RR, Pasceri P, Ellis J. Retrovirus silencing, variegation, extinction, and memory are controlled by a dynamic interplay of multiple epigenetic modifications. *Mol Ther* 2004;10:27–36.
- Klarenbeek PL, de Hair MJH, Doorenspleet ME, van Schaik BDC, Esveldt REE, van de Sande MGH, et al. Inflamed target tissue provides a specific niche for highly expanded T-cell clones in early human autoimmune disease. *Ann Rheum Dis* 2012;71:1088–93.
- Fu Y, Li B, Li Y, Wang M, Yue Y, Xu L, et al. A comprehensive immune repertoire study for patients with pulmonary tuberculosis. *Mol Genet Genomic Med* 2019;7:e00792.
- Dudley ME, Wunderlich JR, Robbins PF, Yang JC, Hwu P, Schwartzentruber DJ, et al. Cancer regression and autoimmunity in patients after clonal repopulation with antitumor lymphocytes. *Science* 2002;298:850–4.
- Hunder NN, Wallen H, Cao J, Hendricks DW, Reilly JZ, Rodmyre R, et al. Treatment of metastatic melanoma with autologous CD4+ T cells against NY-ESO-1. *N Engl J Med* 2008;358:2698–703.
- Burns WR, Zheng Z, Rosenberg SA, Morgan RA. Lack of specific gamma-retroviral vector long terminal repeat promoter silencing in patients receiving genetically engineered lymphocytes and activation upon lymphocyte restimulation. *Blood* 2009;114:2888–99.
- De Ravin SS, Su L, Theobald N, Choi U, Macpherson JL, Poidinger M, et al. Enhancers are major targets for murine leukemia virus vector integration. *J Virol* 2014;88:4504–13.
- Aker M, Tubb J, Miller DG, Stamatoyannopoulos G, Emery DW. Integration bias of gammaretrovirus vectors following transduction and growth of primary mouse hematopoietic progenitor cells with and without selection. *Mol Ther* 2006;14:226–35.
- Chou J, Voong LN, Mortales CL, Towler AMH, Pollack SM, Chen X, et al. Epigenetic modulation to enable antigen-specific T-cell therapy of colorectal cancer. *J Immunother* 2012;35:131–41.
- Pollack SM, Li Y, Blaisdell MJ, Farrar EA, Chou J, Hoch BL, et al. NYESO-1/LAGE-1s and PRAME are targets for antigen specific T cells in chondrosarcoma following treatment with 5-Aza-2-deoxycytidine. *PLoS One* 2012;7:e32165.
- Roth TL, Puig-Saus C, Yu R, Shifrut E, Carnevale J, Li PJ, et al. Reprogramming human T cell function and specificity with non-viral genome targeting. *Nature* 2018;559:405–9.
- Yang L, Baltimore D. Long-term in vivo provision of antigen-specific T cell immunity by programming hematopoietic stem cells. *Proc Natl Acad Sci U S A* 2005;102:4518–23.
- Vatakis DN, Koya RC, Nixon CC, Wei L, Kim SG, Avancena P, et al. Antitumor activity from antigen-specific CD8 T cells generated in vivo from genetically engineered human hematopoietic stem cells. *Proc Natl Acad Sci U S A* 2011;108:E1408–16.
- Pfeifer A, Ikawa M, Dayn Y, Verma IM. Transgenesis by lentiviral vectors: lack of gene silencing in mammalian embryonic stem cells and preimplantation embryos. *Proc Natl Acad Sci U S A* 2002;99:2140–5.
- D'Angelo SP, Melchiori L, Merchant MS, Bernstein D, Glod J, Kaplan R, et al. Antitumor activity associated with prolonged persistence of adoptively transferred NY-ESO-1 (c259)T cells in synovial sarcoma. *Cancer Discov* 2018;8:944–57.
- Yost KE, Satpathy AT, Wells DK, Qi Y, Wang C, Kageyama R, et al. Clonal replacement of tumor-specific T cells following PD-1 blockade. *Nat Med* 2019;25:1251–9.
- Carlson CS, Emerson RO, Sherwood AM, Desmarais C, Chung M-W, Parsons JM, et al. Using synthetic templates to design an unbiased multiplex PCR assay. *Nat Commun* 2013;4:2680.
- Comin-Anduix B, Gualberto A, Glaspy JA, Seja E, Ontiveros M, Reardon DL, et al. Definition of an immunologic response using the major histocompatibility complex tetramer and enzyme-linked immunospot assays. *Clin Cancer Res* 2006;12:107–16.
- Li LC, Dahiya R. MethPrimer: designing primers for methylation PCRs. *Bioinformatics* 2002;18:1427–31.
- Kumaki Y, Oda M, Okano M. QUMA: quantification tool for methylation analysis. *Nucleic Acids Res* 2008;36:W170–5.
- Li H, Handsaker B, Wysoker A, Fennell T, Ruan J, Homer N, et al. The sequence alignment/map format and SAMtools. *Bioinformatics* 2009;25:2078–9.

CANCER DISCOVERY

Epigenetic Suppression of Transgenic T-cell Receptor Expression via Gamma-Retroviral Vector Methylation in Adoptive Cell Transfer Therapy

Theodore S. Nowicki, Colin Farrell, Marco Morselli, et al.

Cancer Discov 2020;10:1645-1653. Published OnlineFirst July 22, 2020.

| | |
|-------------------------------|---|
| Updated version | Access the most recent version of this article at: doi: 10.1158/2159-8290.CD-20-0300 |
| Supplementary Material | Access the most recent supplemental material at: http://cancerdiscovery.aacrjournals.org/content/suppl/2020/07/17/2159-8290.CD-20-0300.DC1 |

| | |
|-----------------------|--|
| Cited articles | This article cites 29 articles, 14 of which you can access for free at: http://cancerdiscovery.aacrjournals.org/content/10/11/1645.full#ref-list-1 |
|-----------------------|--|

| | |
|------------------------|---|
| Citing articles | This article has been cited by 1 HighWire-hosted articles. Access the articles at: http://cancerdiscovery.aacrjournals.org/content/10/11/1645.full#related-urls |
|------------------------|---|

| | |
|----------------------|--|
| E-mail alerts | Sign up to receive free email-alerts related to this article or journal. |
|----------------------|--|

| | |
|-----------------------------------|--|
| Reprints and Subscriptions | To order reprints of this article or to subscribe to the journal, contact the AACR Publications Department at pubs@aacr.org . |
|-----------------------------------|--|

| | |
|--------------------|--|
| Permissions | To request permission to re-use all or part of this article, use this link http://cancerdiscovery.aacrjournals.org/content/10/11/1645 . Click on "Request Permissions" which will take you to the Copyright Clearance Center's (CCC) Rightslink site. |
|--------------------|--|